entropy

MDPI

Article

Conformity, Anticonformity and Polarization of Opinions: Insights from a Mathematical Model of Opinion Dynamics

Tyll Krueger [1], Janusz Szwabiński [2,*] and Tomasz Weron [2]

[1] Department of Control Systems and Mechatronics, Wrocław University of Science and Technology, Wrocław 50-370, Poland; tyll.krueger@pwr.wroc.pl

[2] Faculty of Pure and Applied Mathematics, Wrocław University of Science and Technology, Wrocław 50-370, Poland; tomek.weron@gmail.com

* Correspondence: janusz.szwabinski@pwr.edu.pl; Tel.: +48-71-320-3184

Received: 29 May 2017; Accepted: 18 July 2017; Published: 19 July 2017

Abstract: Understanding and quantifying polarization in social systems is important because of many reasons. It could for instance help to avoid segregation and conflicts in the society or to control polarized debates and predict their outcomes. In this paper, we present a version of the q-voter model of opinion dynamics with two types of responses to social influence: conformity (like in the original q-voter model) and anticonformity. We put the model on a social network with the double-clique topology in order to check how the interplay between those responses impacts the opinion dynamics in a population divided into two antagonistic segments. The model is analyzed analytically, numerically and by means of Monte Carlo simulations. Our results show that the system undergoes two bifurcations as the number of cross-links between cliques changes. Below the first critical point, consensus in the entire system is possible. Thus, two antagonistic cliques may share the same opinion only if they are loosely connected. Above that point, the system ends up in a polarized state.

Keywords: opinion dynamics; social influence; conformity; anticonformity; polarization; agent-based modeling; dynamical systems

1. Introduction

What do affirmative action and gun control [1], same-sex marriage and sexual minority rights [2], abortion [3] stem cell research [4], global warming [5], attitudes toward political candidates [6] or the recent refugee crisis in Europe [7] have in common? All of these keywords are examples of topics known to ignite polarized debates in society. Studying them could thus shed more light on the phenomenon of polarization, which is one of the central issues in the recent opinion dynamics research. Polarization is understood here as a situation in which a group of people is divided into two opposing parties having contrasting positions [8]. It is sometimes referred to as bi-polarization [9] to distinguish it from the so-called group polarization, i.e., the tendency for a group to make decisions that are more extreme than the initial inclination of its members [10,11].

Understanding and quantifying polarization is important because of many reasons. It could for instance help to avoid segregation and conflicts in the society [8] or to control polarized debates and predict their outcomes [12]. There are numerous theories [13–17] and many experimental attempts [18–26] to explain the formation and dynamics of individuals' opinions, including the mechanisms leading to polarization. As far as the theoretical part is concerned, mathematical and computational approaches are dominant in modeling of opinion dynamics [27]. In general, mathematical models allow for some theoretical and/or numerical analysis [28–33]. They usually

make some reasonable assumptions (e.g., a homogeneous and well-mixed population) to simplify the spreading process of opinions and focus on its representation at the macroscopic level. With the appearance of affordable high-performance computers, simulation approaches to opinion dynamics are more and more popular [34–36]. They usually build opinion formation models at the individual level, providing more detailed representation of realities at the cost of higher computational complexity.

Agent-based models are one of the most powerful tools available for theorizing about opinion dynamics [37]. In many cases, they act as in silico laboratories wherein diverse questions can be posed and investigated. There are already several attempts to apply such models to polarization. For instance, French [13], Harary [14] and Abelson [38] showed that consensus must arise in populations whose members are unilaterally connected unless the underlying social network is separated. According to Axelrod [15], local convergence may lead to global polarization. A number of papers has been devoted to explaining polarization within the social balance theory, i.e., by accounting for sentiment in dyadic and/or triadic relations in social networks [39,40]. In other computer experiments, it has been shown that bridges between clusters in a social network (long-range ties) may foster cultural polarization if homophily and assimilation at the micro level are combined with some negative influence, e.g., xenophobia and differentiation [17,41]. Within the information accumulation systems, the probability of reaching consensus has been found to decrease with the total number of interactions between agents that take place in the society [42]. From other studies, it follows that polarization may be also induced by geometry of social ties [43], mass media communication [44] or some external actions of suitable controls (e.g., opinion leadership) [45,46].

Although the aforementioned models are very insightful, we still have some gaps in understanding concerning polarization. One of the recent examples is the impact of new communication channels like websites, blogs and social media on polarization. In particular, social media services are by definition a space for information exchange and discussion. They shrink distances and facilitate communication among people of various backgrounds. There are two competing hypotheses [47]. The first one states that people tend to expose themselves to like-minded points of view and rather avoid dissimilar perspectives. As a consequence, they form more extreme opinions in the direction of their original inclination [48,49], which leads to both group and bi-polarization. Tools such as filtering and recommendation systems built in social media are considered to amplify this tendency. According to the other hypothesis, new media enable people to encounter more diverse views and thus to have balanced opinions on different hot topics [50,51]. The empirical evaluation of these two hypotheses is inconclusive. Some studies have shown that people are more likely to select information sources consistent with their opinions or beliefs [18–21]. Cognitive dissonance, i.e., the mental stress or discomfort experienced by an individual holding two contradictory opinions at the same time, has been identified as one of the possible triggers of such behavior [52,53]. On the other hand, there are some findings that individuals do not avoid information sources representing opposing points of view [22–24]. Some theories state that exposure to dissimilar views may have depolarizing effect, because it stimulates critical thinking [54]. This effect has been observed in a series of experiments [25,26].

Recently, an Ising-type agent-based model of a social system has been presented to study if and how a combination of different responses to social influence may lead to polarization in a segmented network [55]. The model was based on the q-voter model of binary opinion dynamics [34] with an additional type of social response: anticonformity. From the statistical physics point of view, the model falls into the category of quenched disorder models, which are known to be hard to analyze mathematically [56]. In this work, we introduce an annealed version of that model that allows for mathematical treatment. We find a limiting dynamic system for a model of infinite size, which allows us to build the phase portrait of the model and gain some insight into its dynamics. The limiting system is solved numerically. However, we also calculate some of its characteristics analytically. Finally, we show with the help of computer simulations that both the quenched and the annealed models of a finite size converge to the limiting system with the increasing number of agents.

The paper is organized as follows. In the next section, we introduce the model and briefly describe how it differs from the one presented in [55]. Then, we will investigate the model both analytically and numerically. Finally, some conclusions will be presented.

2. Materials and Methods

2.1. Basic Assumptions

We begin with a brief description of the assumptions of the model analyzed in [55]. We choose the q-voter model [34] as our modeling framework. Within the original model, q randomly picked neighbors influence a voter to change his/her opinion. The voter conforms to their opinion if all q neighbors agree. If they are not unanimous, the voter can still flip with a probability ϵ. The unanimity rule is in line with a number of social experiments. For instance, it has been observed that a larger group with a non-unanimous majority is usually less efficient in terms of social influence than a small unanimous group [57,58]. Moreover, Asch found that conformity (i.e., matching attitudes, beliefs and behaviors to group norms) is reduced dramatically by the presence of a social supporter: targets of influence having a partner sharing the same opinion were far more independent when opposed to a seven-person majority than targets without a partner opposed to a three-person majority [59].

From social networks analysis, it follows that the existence of segments within a network may be correlated with polarization [60–62]. We will thus assume that our social network is already modular. For the sake of simplicity, we will put the model on the so-called double-clique topology consisting of two complete graphs (cliques) connected by some cross-links with each other [63]. An example of such a network is shown in Figure 1. It should be emphasized that this is a rather strong assumption, because one actually cannot rule out the opposite possibility that segmentation is induced or intensified by polarization. However, analysis of the casual connection between the network segmentation and the polarization is beyond the scope of this work and will be addressed in a forthcoming paper.

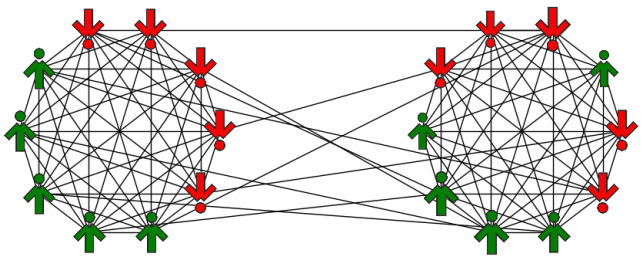

Figure 1. An example of a double-clique network. The network consists of two separate complete graphs (cliques) with some cross-links between them.

The original q-voter model uses conformity, i.e., the act of matching attitudes and opinions to group norms, as the only response to social influence. Other possible types of responses have been described for instance within the diamond model [64–67] and are shown in Figure 2. The anticonformity (i.e., challenging the position or actions of a group) representing negative ties is of particular interest, because from the social balance theories, it follows that both positive and negative ties are needed for polarization to emerge and to prevail [40].Thus, we will add this type of response to our model to check how the interplay between conformity and anticonformity impacts its dynamics.

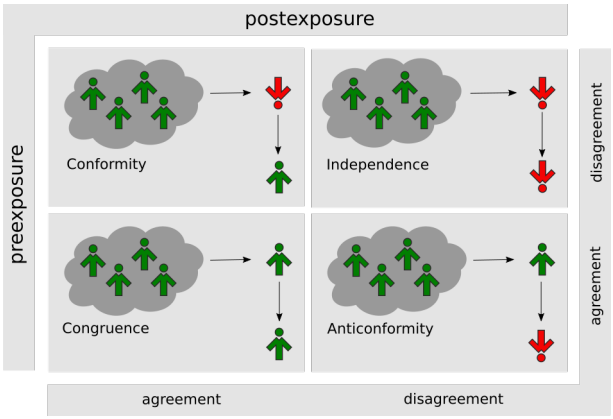

Figure 2. Possible responses to social influence according to the diamond model [64–67]; here, presented within a q-voter model framework with $q = 4$ [34]. The source of influence is a group consisting of unanimous agents (schematically pictured as a cloud). The "up"' and "down"' spins (arrows) represent agents with two different opinions on a single issue.

It is worth noting here that the anticonformity as a type of social response was introduced into binary models of opinion dynamics for the first time probably by Serge Galam, who used the notion of "contrarians" in order to describe agents always adopting opinions opposite to the prevailing choice of others [68]. In his seminal paper, he showed that there exists a critical density of contrarians above which a system always ends up in a bi-polarized state.

We are however aware that the assumption of negative influence is still a subject of intense debate. There are several models able to explain polarization without any kind of negative influence, for example the argument-communication theory of bi-polarization [9] or the bounded-confidence model [16]. Some empirical studies on negative influence do not provide convincing support for this assumption either [69].

There is an important point while speaking about anticonformity: it is relative. It turns out that in many settings, multiple sources of norms are possible. As a consequence, conformity to one source can at the same time be anticonformity to another. For instance, a teenager's conformity to peers is very often anticonformity to his/her parents [66]. Therefore, we will assume within our model that an agent strives for agreement within his own clique and simultaneously anticonforms to individuals from the other clique.

Within the q-voter model, all individuals are characterized by a single dichotomous variable, i.e., the model belongs to the class of binary models. At first glance, this approach may seem unrealistic, because the opinions of individuals on specific subjects are expected to vary gradually. Therefore, they should be rather represented by continuous variables [9,13,14,16]. However, from empirical findings, it follows that the distribution of opinions on important issues measured on some multivalued scale is often bimodal and peaked at extreme values [70,71]. Moreover, many data on social networks are characterized by a semantic unicity, meaning that opinions and interactions of networks' members are restricted to a single domain or topic [72]. Very often, those opinions may be interpreted as simple "yes"/"no", "in favor of"/"against" or "adopted"/"not adopted" answers [73]. In other words, in some situations, the most important characteristics of the system under investigation may be already captured by the relatively simple models of binary opinions.

2.2. The "Old" (Quenched Disorder) Model

In this section, we recall the model introduced in [55]. We consider a set of $2N$ agents, each of whom has an opinion on some issue that at any given time can take one of two values: $S_i = -1$ or $S_i = 1$ for $i = 1, 2, \ldots, 2N$. We will sometimes call these agents spinsons to reflect their dichotomous

nature originating in spin models of statistical physics and humanly features and interpretation (*spinson* = *spin* + *person*) [35,74].

We put our agents on a double-clique network. It consists of two complete graphs of N nodes connected with $L \times N^2$ cross-links (Figure 1). The parameter L is the fraction of the existing cross-links and N^2 their maximum number. The cross-links between the cliques are chosen randomly and the resulting network does not evolve in time during simulation. Thus, from the statistical physics' point of view, the model belongs to the class of models with quenched disorder [75].

We will assume that a spinson strives for agreement within his/her own clique (conformity) and simultaneously challenges the opinions of individuals from the other clique (anticonformity). In other words, we link the type of social response of agents with their group identity. To account for the possibility of acting as both conformist and anticonformist at the same time within the q-voter model, we introduce the notion of signals and slightly alter the concept of unanimity of the influence group. A signal is just a state of the neighbor when coming from the spinson's clique or its inverted state otherwise. The target of influence changes its opinion only if all members of the influence group emit the same signal. No other modification of the q-voter framework are needed to account for anticonformity.

We use Monte Carlo simulation techniques with a random sequential updating scheme to investigate the model. Each Monte Carlo step in our simulations consists of $2 \times N$ elementary events, each of which may be divided into the following sub-steps:

1. Pick a target spinson at random (uniformly from $2N$ nodes).
2. Build its influence group by randomly choosing q neighboring agents.
3. Convert the states of the neighbors into signals that may be received by the target. Assume that the signals of the neighbors from the target's clique are equal to their states. Invert the states when from the other clique.
4. Calculate the total signal of the influence group by summing up individual signals of its members.
5. If the total signal is equal to $\pm q$ (i.e., all group members emit the same signal), the target changes its opinion accordingly. Otherwise, nothing happens.

Thus, our model is nothing but a modification of the q-voter with $\epsilon = 0$ and an additional social response of spinsons. You may refer to [55] for further details of the model.

2.3. New ("Annealed") Version of the Model

In the model described in the previous section, the cross-links between the cliques are generated randomly at the beginning of a simulation and remain fixed while the system evolves in time. If the number of cross-links is smaller than their maximum number N^2 (i.e., $L < 1$), some agents may have no connections to the other clique, some others, multiple ones. In other words, the agents may differ from each other because of the distribution of links between the cliques. While it can be handled with ease within a computer simulation, this feature constitutes usually a challenge for mathematical modeling due to the necessity to perform a quenched average over the disorder [56]. Thus, we decided to modify the model slightly for simpler mathematical treatment.

Most of the assumptions presented earlier in this section hold, i.e., we consider $2N$ agents living on a double-clique network. Each agent may be in one of the states $\{+1, -1\}$ representing its opinion on some issue. It seeks for agreement within its own clique (conformity) and simultaneously anticonforms with respect to individuals from the other clique (anticonformity). Additionally, it changes its opinion if the members of an influence group emit the same signal. Just to recall, a signal is just a state of the neighbor when coming from the agents's clique or its inverted state otherwise.

If the size N of each clique is large enough, then the number of links within a single clique is given by:

$$\frac{(N-1)N}{2} \approx \frac{N^2}{2}. \tag{1}$$

With the number of cross-connections equal to $L \times N^2$, the quantity:

$$p = \frac{LN^2}{LN^2 + 2 \times \frac{N^2}{2}} = \frac{L}{1+L} \tag{2}$$

gives us the probability of choosing one cross-link out of all edges in the double-clique network. Assuming that every agent from one clique is connected with probability p with an agent from the other clique, and with probability $1-p$ with an agent from its own clique, we arrive at the new version of our model. Technically, this approximation is nothing but an average of the original (quenched disorder) model over different configurations of cross-links in the network. Thus, it corresponds to annealed models from statistical physics [76].

Step 2 from the update rules of the model defined in Section 2.2 requires some adjustments:

1. Pick a target spinson at random (uniformly from $2N$ nodes).
2. Build its influence group by randomly choosing q agents. In the quenched disorder model, we simply followed 4 randomly-chosen links of the target to achieve that. Due to the setup of that model, some targets usually had no cross-connections, some others-multiple ones. Now, the situation is different: each target has the same probability of being cross-connected, and the actual links to other agents have to be built first. Thus, for each member of the influence group, we decide first which clique it will belong to (with probability $1-p$ to the target's clique, with p to the other one). Then, we choose the member randomly from the appropriate clique (see Figure 3).
3. Convert the states of the group members into signals.
4. Calculate the total signal of the influence group.
5. If the total signal is equal to $\pm q$ (i.e., all group members emit the same signal), the target changes its opinion accordingly. Otherwise, nothing happens.

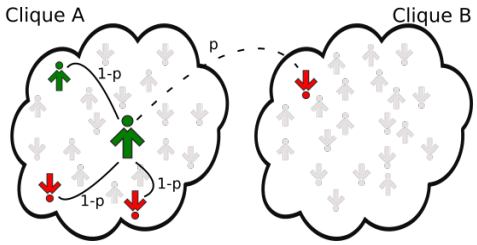

Figure 3. Finding the influence group in the new version of the model. Each link of the target (the big green agent in the middle of Clique A) is chosen independently. With probability p, it may point to an agent from the other clique (dashed line), with probability $1-p$, from the target's one (solid lines). See Step 2 of the update procedure defined in Section 2.3 for more explanation.

It should be noted that a similar model, but with a broken symmetry between the cliques, was used in both the quenched and the annealed version to explain recurring fashion cycles [77].

Let us denote the state of the i-th agent at the discrete time τ by $S_i(\tau)$. There are two natural quantities that fully describe the state of the system: the concentration of agents in state $+1$ and the average opinion (magnetization in physical systems) [35]. The concentration at time τ is defined as:

$$c(\tau) = \frac{N^{\uparrow}(\tau)}{2N} \quad \rightarrow \quad c(\tau) \in [0,1], \tag{3}$$

where $N^{\uparrow}(\tau)$ is the number of agents in state $+1$ at time τ. The average opinion is given by:

$$m(\tau) = \frac{N^{\uparrow}(\tau) - N^{\downarrow}(\tau)}{2N} \quad \rightarrow \quad m(\tau) \in [-1,1]. \tag{4}$$

Please note that there is a simple relation between these two quantities:

$$m(\tau) = 2c(\tau) - 1. \tag{5}$$

Thus, it actually does not matter which one will be chosen for representation of the state of the system. For the sake of convenience, we will usually work with the concentration below. However, some of the results will be transformed to average opinions to allow for comparisons with the findings from [55].

In order to easily detect polarized states in the system (i.e., all agents in state $+1$ in one clique and in state -1 in the other), we will often calculate the concentration separately for each clique:

$$c_X(\tau) = \frac{N_X^{\uparrow}(\tau)}{N_X} \quad , X = A, B, \tag{6}$$

where A and B are the labels of the cliques.

The interpretation of c_X is as follows:

- $c_X = 1$: positive consensus in clique X, i.e., all agents in that clique are in state $+1$,
- $\frac{1}{2} < c_X < 1$: partial positive ordering in clique X, i.e., the majority of agents is in state $+1$,
- $c_X = \frac{1}{2}$: no ordering in clique X, i.e., the numbers of agents in state $+1$ and -1 are equal,
- $0 < c_X < \frac{1}{2}$: partial negative ordering in clique X, i.e., the majority of agents are in state -1,
- $c_X = 0$: negative consensus in clique X, i.e., all agents in that clique are in state -1.

2.3.1. Transition Probabilities

In each elementary time step, the number of agents in state $+1$ in one clique, say A, can increase by 1 only if:

1. a target from clique A is chosen (probability $1/2$),
2. the target is in state -1 (probability $1 - c_A$),
3. it flips, i.e., an influence group emitting signal $+q$ is chosen.

We can immediately write down the transition probability for such an event:

$$\Pr\left\{N_A^{\uparrow}(t + \Delta_N) = N_A^{\uparrow}(t) + 1\right\} = \frac{1}{2}\left(1 - c_A(t)\right)\left[(1-p)\, c_A(t) + p\left(1 - c_B(t)\right)\right]^q. \tag{7}$$

We have introduced here a scaled time $t = \frac{\tau}{2N}$ and a scaled time step $\Delta_N = \frac{1}{2N}$. We will use them below to derive a limiting dynamical system for the model.

Moreover, one can easily check that the term of the form $(u + v)^q$ in the above equation is just the generating function for the probabilities of those compositions of q members of an influence group that can cause an opinion switch event (see Figure 4).

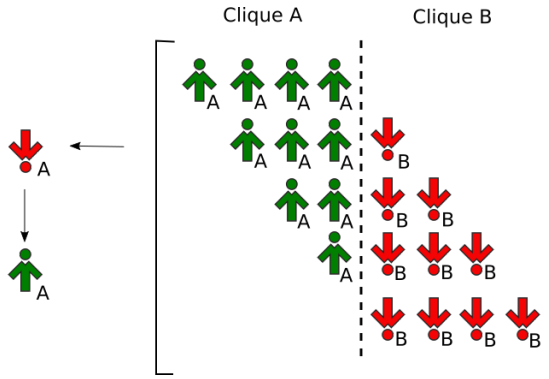

Figure 4. Possible choices of the influence group in case $q = 4$ that lead to an opinion flip of a spinson in Clique Abeing initially in state $S = -1$. See [55] for further details.

Similarly, the number of spinsons in state $+1$ in Clique A decreases by 1 if:

1. a target from clique A is chosen (probability $1/2$),
2. the target is in state $+1$ (probability c_A),
3. it flips, i.e., an influence group emitting signal $-q$ is chosen.

These conditions lead to the following transition probability:

$$\Pr\left\{N_A^{\uparrow}\left(t+\Delta_N\right)=N_A^{\uparrow}\left(t\right)-1\right\}=\frac{1}{2}c_A\left(t\right)\left[\left(1-p\right)\left(1-c_A\left(t\right)\right)+pc_B\left(t\right)\right]^q. \tag{8}$$

It is also possible that the number of agents in state $+1$ remains unchanged in the elementary time step. The probability of this event is simply given by:

$$\Pr\left\{N_A^{\uparrow}\left(t+\Delta_N\right)=N_A^{\uparrow}\left(t\right)\right\}=1-\Pr\left\{N_A^{\uparrow}\left(t+\Delta_N\right)=N_A^{\uparrow}\left(t\right)+1\right\}-\Pr\left\{N_A^{\uparrow}\left(t+\Delta_N\right)=N_A^{\uparrow}\left(t\right)-1\right\}. \tag{9}$$

After repeating analogous considerations for Clique B, we get:

$$\begin{aligned}
\Pr\left\{N_B^{\uparrow}\left(t+\Delta_N\right)=N_B^{\uparrow}\left(t\right)+1\right\} &= \frac{1}{2}\left(1-c_B\left(t\right)\right)\left[\left(1-p\right)c_B\left(t\right)+p\left(1-c_A\left(t\right)\right)\right]^q \\
\Pr\left\{N_B^{\uparrow}\left(t+\Delta_N\right)=N_B^{\uparrow}\left(t\right)-1\right\} &= \frac{1}{2}c_B\left(t\right)\left[\left(1-p\right)\left(1-c_B\left(t\right)\right)+pc_A\left(t\right)\right]^q \\
\Pr\left\{N_B^{\uparrow}\left(t+\Delta_N\right)=N_B^{\uparrow}\left(t\right)\right\} &= 1-\Pr\left\{N_B^{\uparrow}\left(t+\Delta_N\right)=N_B^{\uparrow}\left(t\right)+1\right\}-\Pr\left\{N_B^{\uparrow}\left(t+\Delta_N\right)=N_B^{\uparrow}\left(t\right)-1\right\}
\end{aligned} \tag{10}$$

Thus, given the states of the cliques at time t, the expectations for the numbers of agents in state $+1$ at time $t+\Delta_N$ are given by the following expressions:

$$\begin{aligned}
E\left(N_A^{\uparrow}\left(t+\Delta_N\right)\right) &= N_A^{\uparrow}\left(t\right)+\frac{1}{2}\left(1-c_A\left(t\right)\right)\left[\bar{p}c_A\left(t\right)+p\left(1-c_B\left(t\right)\right)\right]^q \\
&\quad -\frac{1}{2}c_A\left(t\right)\left[\bar{p}\left(1-c_A\left(t\right)\right)+pc_B\left(t\right)\right]^q \\
E\left(N_B^{\uparrow}\left(t+\Delta_N\right)\right) &= N_B^{\uparrow}\left(t\right)+\frac{1}{2}\left(1-c_B\left(t\right)\right)\left[\bar{p}c_B\left(t\right)+p\left(1-c_A\left(t\right)\right)\right]^q \\
&\quad -\frac{1}{2}c_B\left(t\right)\left[\bar{p}\left(1-c_B\left(t\right)\right)+pc_A\left(t\right)\right]^q
\end{aligned} \tag{11}$$

The abbreviation $\bar{p}=1-p$ was used in the above formulas.

2.3.2. Asymptotic Dynamical System

We would like to derive from Equation (11) a limiting dynamical system for $N\to\infty$ in scaled time $t=\frac{\tau}{2N}$. Let us first divide the above equations by N:

$$\begin{aligned}
E\left(c_A\left(t+\Delta_N\right)\right)-c_A\left(t\right) &= \Delta_N\left(1-c_A\left(t\right)\right)\left[\bar{p}c_A\left(t\right)+p\left(1-c_B\left(t\right)\right)\right]^q \\
&\quad -\Delta_N c_A\left(t\right)\left[\bar{p}\left(1-c_A\left(t\right)\right)+pc_B\left(t\right)\right]^q \\
E\left(c_B\left(t+\Delta_N\right)\right)-c_B\left(t\right) &= \Delta_N\left(1-c_B\left(t\right)\right)\left[\bar{p}c_B\left(t\right)+p\left(1-c_A\left(t\right)\right)\right]^q \\
&\quad -\Delta_N c_B\left(t\right)\left[\bar{p}\left(1-c_B\left(t\right)\right)+pc_A\left(t\right)\right]^q
\end{aligned} \tag{12}$$

It is very likely that in the limit $N\to\infty$, the random variables $c_i=\frac{N_i^{\uparrow}}{N}$ localize and hence become almost surely equal to their expectations. We get:

$$\begin{aligned}
\frac{c_A\left(t+\Delta_N\right)-c_A\left(t\right)}{\Delta_N} &= \left(1-c_A\left(t\right)\right)\left[\bar{p}c_A\left(t\right)+p\left(1-c_B\left(t\right)\right)\right]^q-c_A\left(t\right)\left[\bar{p}\left(1-c_A\left(t\right)\right)+pc_B\left(t\right)\right]^q \\
\frac{c_B\left(t+\Delta_N\right)-c_B\left(t\right)}{\Delta_N} &= \left(1-c_B\left(t\right)\right)\left[\bar{p}c_B\left(t\right)+p\left(1-c_A\left(t\right)\right)\right]^q-c_B\left(t\right)\left[\bar{p}\left(1-c_B\left(t\right)\right)+pc_A\left(t\right)\right]^q
\end{aligned} \tag{13}$$

Taking the limit $N \to \infty$ and denoting the limiting variables c_A and c_B by x and y, we arrive at:

$$\begin{aligned} x' &= (1-x)\left(\bar{p}x + p\left(1-y\right)\right)^q - x\left(\bar{p}\left(1-x\right) + py\right)^q, \\ y' &= (1-y)\left(\bar{p}y + p\left(1-x\right)\right)^q - y\left(\bar{p}\left(1-y\right) + px\right)^q. \end{aligned} \tag{14}$$

2.3.3. Annealed Model as a Birth-Death Process

According to Equations (7)–(10), we have only two types of state transitions in each clique: "births", which increase the state variable by one, i.e., $N_X^{\uparrow} \to N_X^{\uparrow} + 1$ ($X = A, B$), and "deaths", which decrease it by one, $N_X^{\uparrow} \to N_X^{\uparrow} - 1$. Thus, our model may be seen as two coupled birth-death processes [78]. Since such a process is relatively easy to simulate, we will use it as an additional benchmark while comparing the results for the quenched disorder and annealed models.

3. Results

All results presented in this section were obtained via symbolic and numerical calculations by making use of Python's scientific stack [79]. Python codes needed to reproduce some of them may be found in the Supplementary Materials.

Although we will often use the case $q = 3$ for presenting the results, there is no particular reason for choosing this value. We considered in our analysis influence groups of sizes ranging from 1–6. The upper bound of the group size was motivated by the conformity experiments by Asch [59]. Qualitatively, the results turned out to be independent of the actual value of q. However, with increasing q, the critical points were shifted towards higher values of the interaction parameter p (see Figure 5).

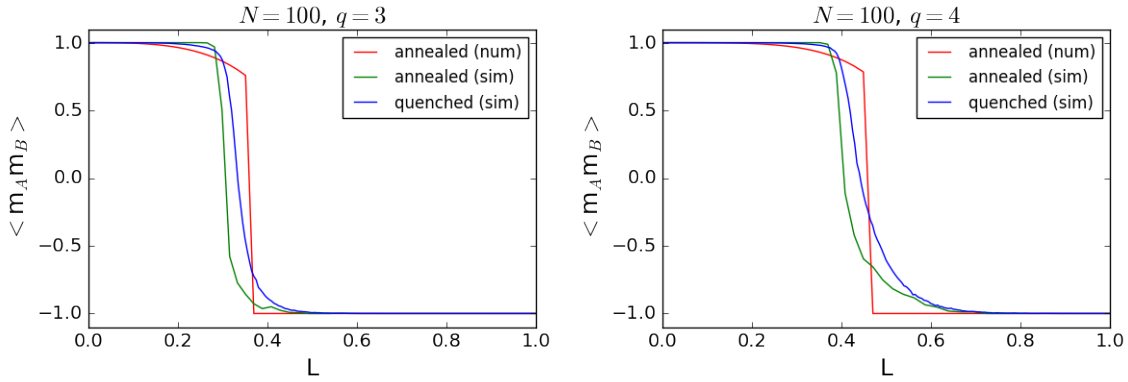

Figure 5. Correlation between cliques as a function of the fraction of cross-links L for $q = 3$ (left plot) and $q = 4$ (right plot). Simulation results of the quenched disorder model (label "quenched (sim)" in the plots) taken from [55] are compared with the numerical solution ("annealed (num)") of the asymptotic dynamical system given by Equation (15), as well as with the simulation of the annealed model as a birth-death process ("annealed (sim)"). Both simulations were performed for a finite size system ($N = 100$ agents in each clique). Despite the differences between the models, the agreement between them is quite good. In particular, for both values of q the transition from consensus to polarization sets in at similar values of L.

3.1. Direction Fields and Stationary Points

Our goal is to investigate the dynamical system given by Equation (14),

$$\begin{aligned} x' &= (1-x)\left(\bar{p}x + p\left(1-y\right)\right)^q - x\left(\bar{p}\left(1-x\right) + py\right)^q, \\ y' &= (1-y)\left(\bar{p}y + p\left(1-x\right)\right)^q - y\left(\bar{p}\left(1-y\right) + px\right)^q. \end{aligned} \tag{15}$$

It is customary to start such an analysis by plotting direction fields in the state space of the system [80]. Examples of the fields for $q = 3$ and two values of the parameter p are shown in Figure 6. As a remainder: the solution trajectory through a given initial state is a curve in the state space, which at every point is tangent to the field at that point.

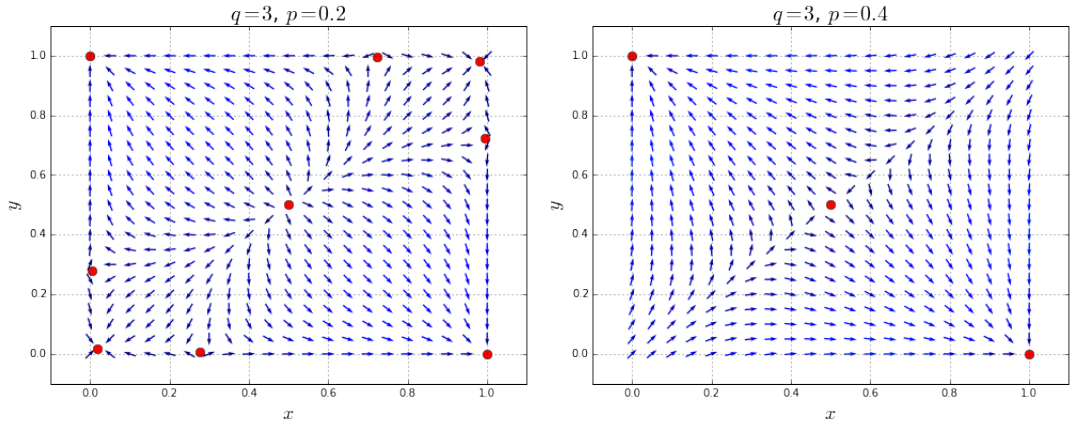

Figure 6. Direction field of the dynamical system (15) for $q = 3$ and two different values of the interaction parameter p: $p = 0.2$ (left plot) and $p = 0.4$ (right plot). Red dots indicate stationary points of the system. The parameters q and p are the size of the influence group and the probability of being connected to an agent from the other clique, respectively.

Several things are immediately clear from the picture shown in the figure. At $p = 0.2$, the flows in the state plane suggest that there are nine stationary points (already marked with red dots). Some of these points are easy to classify. For instance, there are two attractors (i.e., points toward which the system tends to evolve for a wide variety of initial conditions) at $(0, 1)$ and $(1, 0)$ corresponding to a polarized state of the system, i.e., all agents in one clique are in state $+1$ and in the other—in state -1. Moreover, there are two other symmetric attractors close to the coordinates $(0, 0)$ and $(1, 1)$. It seems that (almost) complete consensus is possible in our system for some initial configurations, at least for that particular value of p. The point $(0.5, 0.5)$ is a repeller (the system tends to evolve away from it), and the remaining four points seem to be hyperbolic (near such points, the orbits of a two-dimensional, non-dissipative system resemble hyperbolas).

At $p = 0.4$ (right plot in Figure 6), all hyperbolic points and the symmetric attractors disappear. The point $(0.5, 0.5)$ becomes hyperbolic. The only remaining attractors are $(0, 1)$ and $(1, 0)$. Hence, for higher values of p, the polarization of the system is the only possible asymptotic state. It should be noted that these findings recapture the results from [55].

To find the exact coordinates of the system, we just set x' and y' equal to zero in Equation (15) and solve the resulting set of equations with respect to x and y,

$$\begin{aligned} 0 &= (1-x)\left(\bar{p}x + p\left(1-y\right)\right)^q - x\left(\bar{p}\left(1-x\right) + py\right)^q, \\ 0 &= (1-y)\left(\bar{p}y + p\left(1-x\right)\right)^q - y\left(\bar{p}\left(1-y\right) + px\right)^q. \end{aligned} \tag{16}$$

For $p = 0.2$ and $q = 3$, we get:

$$\begin{aligned} &P_1 = (0,1), \;\; P_2 = (1,0) \\ &C_1 = (0.019, 0.019), \;\; C_2 = (0.981, 0.981) \\ &R_1 = (0.5, 0.5) \\ &U_1 = (0.005, 0.277), \;\; U_2 = (0.277, 0.005) \\ &U_3 = (0.722, 0.995), \;\; U_4 = (0.995, 0.722) \end{aligned} \tag{17}$$

The linear stability analysis of these points reveals that indeed P_1, P_2, C_1 and C_2 are stable equilibria, R is a repeller and the remaining points are hyperbolic ones, in agreement with our analysis of the direction field in Figure 6.

Similarly, for $p = 0.4$ and $q = 3$, we have:

$$P_1 = (0, 1), \quad P_2 = (1, 0) \tag{18}$$

$$R_1 = (0.5, 0.5) \tag{19}$$

As before, P_1 and P_2 are stable, but R_1 is now hyperbolic. The remaining points disappeared (they became complex).

If we repeat the above calculations for other values of the parameter p and plot the results, we get a bifurcation diagram showing how the dynamics of the system changes with p, i.e., with increasing degree of anticonformity in the system. The plot of the x coordinates of the fixed points as functions of p is shown in Figure 7. The picture for the y coordinates would look the same (but with rearranged labels of the unstable points U_i).

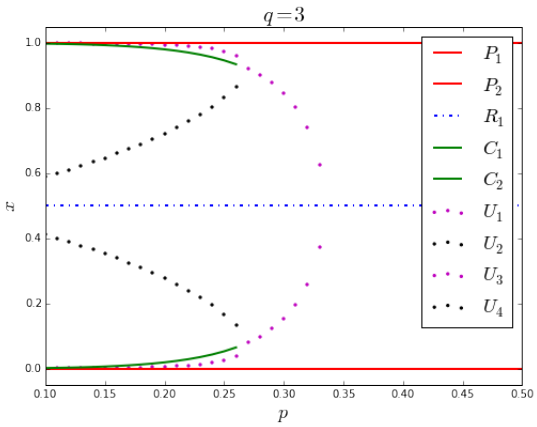

Figure 7. Bifurcation diagram of the system given by Equation (15) for $q = 3$. Solid lines indicate stable fixed points, the remaining ones, repellers and hyperbolic equilibria. At small values of p, the system has four attractors: P_1 and P_2 correspond to asymptotic polarization, C_1 and C_2 to consensus. There is also a repeller R_1 and four hyperbolic points U_1–U_4. As p increases, a bifurcation happens at $p^* \simeq 0.26$. The four hyperbolic non-symmetric points U_1–U_4 disappear, and the consensus equilibria C_1 and C_2 become hyperbolic. With the further increase of p, the symmetric points eventually disappear, and the repeller R_1 becomes hyperbolic.

Stable equilibria are indicated with solid lines. We see that the system has two attractors $P_1 = (0, 1)$ and $P_2 = (1, 0)$, as well as the unstable point $R_1 = (0.5, 0.5)$ as stationary solutions independently of p. However, the system undergoes two phase transitions. At $p_1^\star \simeq 0.26$ the hyperbolic points U_1–U_4 disappear, and the nontrivial symmetric fixed points C_1 and C_2 become hyperbolic. At $p_2^\star \simeq 0.32$, these symmetric points disappear, as well.

The above results were obtained numerically. However, in the special case of $q = 2$, one can find both critical values of p analytically. For a general value of q, an analytical computation of the second critical point is possible, as well. We present corresponding calculations in Appendices B and C.

3.2. Time Evolution of the Asymptotic System

The time evolution of our dynamical system for two different values of p is shown in Figure 8.

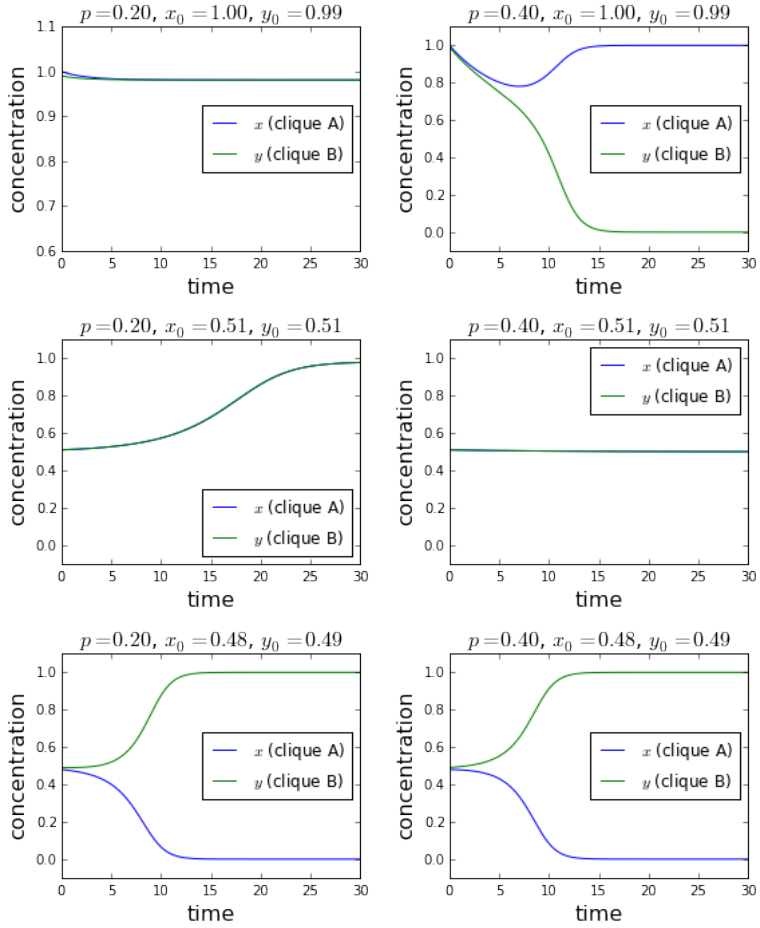

Figure 8. Time evolution of the dynamical system given by Equation (15) for two different values of the parameter p: 0.2 (left column) and 0.4 (right column). The initial concentrations of spinsons in state $+1$ in Clique A (i.e., x_0) and Clique B (y_0) are given in the titles of the plots. The size of the influence group q was set to three in all calculations.

The set (15) of ordinary differential equations was solved numerically in Python by making use of the *odeint* function from the SciPy package [79].

As already known from Figures 6 and 7, at $p = 0.2$, our system may end up either in the polarized state (i.e., P_1 or P_2) or in the consensus one (C_1 or C_2) depending on the initial conditions for the concentrations of $+1$ spinsons. We see that the results shown in the left column of Figure 8 are in line with these findings. If for instance the starting point is the total positive consensus in Clique A ($x_0 = 1.00$) and almost total consensus in Clique B ($y_0 = 0.99$), then the system ends up in state $C_2 = (0.981, 0.981)$, representing consensus in the entire system (top left plot in Figure 8). In this case, the anticonformistic links between cliques, the number of which is represented by p, lead only to a tiny decrease of the initial concentrations of $+1$ agents in both cliques. If the initial conditions are close to the repeller R_1 and symmetric (i.e., we start from a point on the diagonal in the state plane, which means that there is (almost) no ordering in each clique), then again, the system reaches the consensus state (middle left plot). However, a small deviation from the diagonal pushes the system towards the polarized state (bottom left).

As we see, the behavior for $p = 0.4$ is different. The system usually ends up in the polarized state (top and middle right plots in Figure 8). The only exceptions are initial conditions along the diagonal in the state plane (x, y). Since R_1 is now not a repeller, but a hyperbolic fixed point, the system is pushed towards it in this case (bottom right plot). Again, this is in agreement with the direction field shown in Figure 6.

3.3. Basins of Attraction

Attractors of every dynamical system are surrounded by a basin of attraction representing the set of initial conditions in the state space whose orbits approach the attractor as time goes to infinity. In the previous paragraph, we have seen already examples of initial conditions belonging to the basins of the polarization equilibria (P_1 or P_2) and the consensus ones (C_1 or C_2) (see Figure 8). Now, we would like to quantify the shapes of the basins of different attractors of our system. Of particular interest in a model with segmentation and negative ties are the basins of the consensus states, since in such a setting, one intuitively expects polarization as the natural asymptotic state.

Since it is not possible to calculate the shapes analytically, we will resort to numerical methods again. For that purpose, we create first a grid in the state plane (x, y) with both coordinates varying from 0.0–1.0 with step 0.01. The points on the grid represent different initial conditions uniformly distributed in the whole state plane. Then, we solve the dynamical system (15) for each grid point and check what attractor the solution is converging to at long evolution times. Results for $p = 0.2$ and $p = 0.4$ are presented in Figure 9. As often in this paper, the parameter q was set to three in the whole procedure.

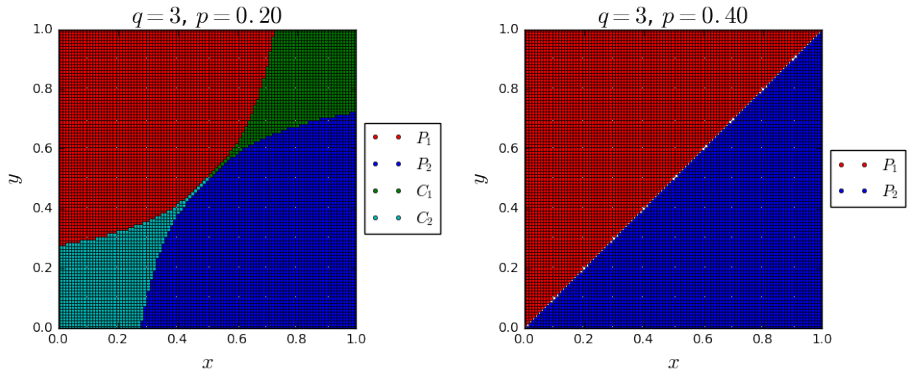

Figure 9. Basins of attraction at two different values of p, 0.2 (left plot) and 0.4 (right plot). Each point in the state plane corresponds to an initial condition. Its color indicates the attractor, to which a solution is converging. The coordinates of the attractors are defined in Equations (17) and (18). Boundaries between the basins are formed by stable manifolds of the hyperbolic points U_1–U_4 (left plot) or of the point R_1 (right plot).

For $p = 0.2$ (left plot in Figure 9), the whole state plane is divided into the basins of four attractors: P_1, P_2, C_1 and C_2. Their coordinates are defined in Equation (17). Surprisingly, the basins of both positive (C_2) and negative (C_1) consensus are relatively large. Thus, if the number of negative connections between the cliques is small, the consensus may still by reached in a double-clique network for a range of initial conditions. It is worth mentioning that the boundaries between the basins observed in the plot are formed by the stable manifolds of non-symmetric hyperbolic points U_1–U_4.

The picture at $p = 0.4$ (right plot in Figure 9) is simpler. Consensus is no longer possible and the whole state plane is divided into the basins of two polarization points P_1 and P_2 (see Equation (18) for their coordinates). The boundary between them corresponds to the stable manifold of R_1, which is now hyperbolic.

3.4. Correlation between Cliques

All results presented up to this point indicate that some sort of a competition between conformity and anticonformity may be responsible for substantial changes in the dynamics of the model. To elaborate on that issue, we will look at the product of the final states of the cliques,

$$c_A^\infty c_B^\infty = x^\infty y^\infty, \tag{20}$$

as a function of p at different values of q. We will call this quantity a correlation between the cliques. To allow for comparisons with the results presented in [55] we will focus our attention on the total positive consensus $x_0, y_0 = 1.0$ as the initial condition. It is referred to as Scenario I in [55] and corresponds to the following situation: two cliques with a natural tendency to disagree with each other evolve at first independently. They get in touch by chance and establish some cross-links to the other group once they both reached consensus on a given issue.

Results for the correlation between the cliques are presented in Figure 10.

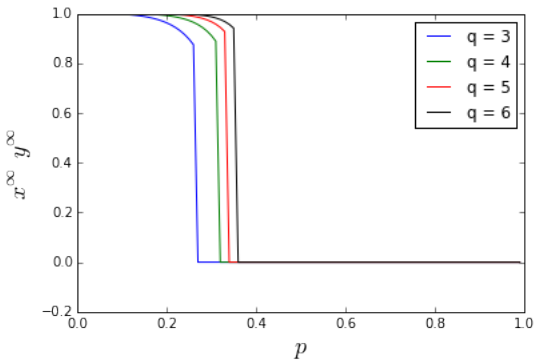

Figure 10. Correlation $x^\infty y^\infty$ between final states of the cliques as a function of p for different values of q. Below the bifurcation (critical) value of p, consensus between cliques is possible. With increasing p, the consensus is slightly diminished because of the increasing role of the negative ties between the cliques. Above the bifurcation point, only polarization is possible in the system.

For values of p smaller than a critical value ($\simeq 0.267$ for $q = 3$), both cliques always end up in positive consensus. In other words, in this regime, the intra-clique conformity wins with the inter-clique anticonformity, and both communities are able to maintain their initial positive consensus. If the value of p is larger than the critical one, the anticonformity-induced effects take over, and the whole system ends up in a polarized state. Moreover, the critical point shifts with increasing q towards higher values of p (see Table 1 for more details). Thus, the bigger the influence group, the more cross-links are needed to polarize the society.

Table 1. The values of p at the bifurcation point for different values of q.

q	3	4	5	6
p^*	0.267	0.311	0.339	0.359

Let us compare the above results with the model presented in [55]. For that purpose, we have to convert the concentrations of agents in state $+1$ in each clique into average opinions according to Equation (5) and to transform the probability p of being connected to other clique into the number of cross-links L. We obtain the transformation formula immediately from Equation (2):

$$L = \frac{p}{1-p} \tag{21}$$

The comparisons for two different values of q are shown in Figure 5.

The agreement of the results is quite good, despite the differences between the models and the fact that the numerical solution for the annealed model was obtained for an infinite system, whereas the simulations were performed for only $N = 100$ agents in each clique. Most notably, the transition from consensus to polarization sets in at similar values of L in both models.

Some of the discrepancies between the numerical results for the annealed model and the simulation results for the quenched disorder one are due to the finite system size of the quenched

disorder model and the stochastic nature of its simulation. Indeed, the agreement between models is even better, if we leave the numerical solution out of consideration for a moment and concentrate only on the simulation results in both cases. Moreover, as follows from Figure 11, the differences between the models decrease with increasing system size. Thus, for $N \to \infty$ both variants of the model will probably converge to each other.

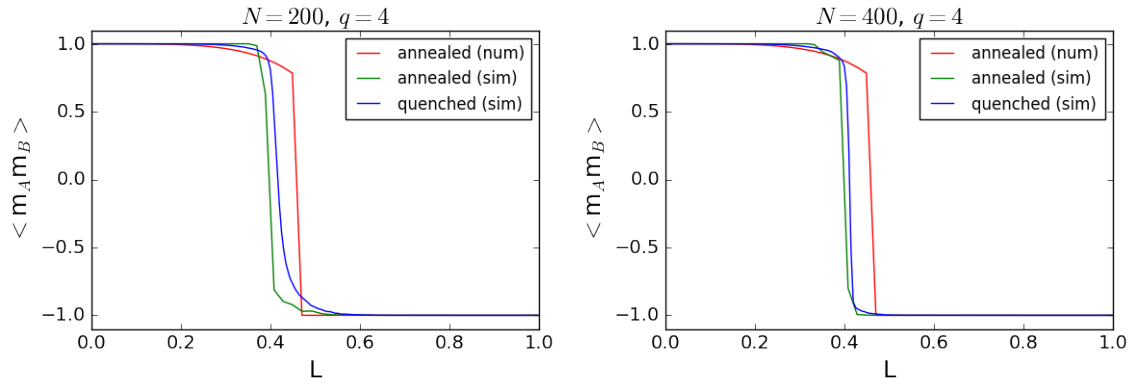

Figure 11. Correlation between cliques as a function of the fraction of cross-links L for $q = 4$ and two different system sizes: $N = 200$(left plot) and $N = 400$ (right plot). See the caption of Figure 5 for an explanation of the labels. The differences between simulation results for both models decrease with increasing system size.

4. Discussion

Due to the computational complexity of the Monte Carlo simulation approach to agent-based models, we were able to investigate only a few distinct initial conditions in [55]. In this paper, thanks to a slight modification of the model, we could analyze it mathematically and therefore explore the whole state plane.

Again, our results indicate that the interplay between conformity and anticonformity may lead to a polarized state of the system. We now have however a much better understanding of the conditions necessary to arrive at consensus, and we have determined regimes in which polarization takes over. Thus, the present results complete the analysis started in [55]. The most important message of the study is that consensus between two antagonistic communities is possible only if they are loosely connected with each other.

It should be noted that similar results have been achieved by Shin and Lorenz [42] within the information accumulation system model of continuous opinion dynamics. The authors found that the convergence of two internally highly connected communities with a comparably low number of cross-links to the same opinion is less possible the more overall interaction between agents takes place.

Explosive growth in Internet-mediated communication facilitates the exchange of opinions between people, both passively and actively [81]. Within the language of our model, this means that modern communication tools like Facebook and Twitter increase the number of links between people in general and between members of differently-minded cliques in particular. Our results imply that if the fraction of cross-links (i.e., the value of p) between such cliques exceeds some critical value, then the polarized state is the only attractor of the system. In real social systems, the situation is of course more complicated, because the cliques interact not only with each other, but with other actors, as well. However, our results may indicate one of the possible mechanisms for the omnipresence of polarization in social media. Paradoxically, the often criticized "filter bubbles" on Facebook or Google [82], which separate users from information (people) that disagrees with their viewpoints, may help to weaken the problem with bi-polarization and to maintain overall consensus, because they reduce the fraction of cross-links between cliques (the discussion of negative effects of "filter bubbles" on the society is beyond the scope of this work).

As far as potential extensions to our model are concerned, the suggestions given in our previous paper still hold. For instance, it could be very informative to check how robust the model is to the introduction of noise, because it is already known that including noise in models of opinion dynamics may significantly change their predictions [83]. Another interesting aspect worth addressing in future studies is the casual connection between the network segmentation and the polarization.

Acknowledgments: This work was partially supported by funds from the Polish National Science Centre (NCN) through Grant No. 2013/11/B/HS4/01061.

Author Contributions: Tyll Krueger and Janusz Szwabiński conceived of and designed the experiments. Tyll Krueger performed the formal analysis of the annealed model. Tomasz Weron implemented the models and ran the computer simulations. Janusz Szwabiński analyzed the annealed model numerically. Tomasz Weron and Janusz Szwabiński compiled and visualized the results. Janusz Szwabiński wrote the paper.

Conflicts of Interest: The authors declare no conflict of interest.

Appendix A. Critical Values of p in Case $q = 2$

From the analysis presented in the main text (see Section 3.1), it follows that the system undergoes two phase transitions. At the first critical point, four hyperbolic nonsymmetric fixed points disappear, and the nontrivial symmetric equilibria become hyperbolic. At the second critical point, these symmetric points disappear, as well.

Our goal is to find both critical values of p analytically in the special case $q = 2$. We will proceed by first computing the coordinates of the nontrivial symmetric fixed points as functions of p. Then, we find coordinates of a symmetric point, at which the largest eigenvalue of the Jacobian is equal to zero. Combining these two results will give us the critical value of the first transition. The second phase transition occurs at a value of p, for which both symmetric points disappear (i.e., they become complex).

For computing the nontrivial symmetric fixed points, we put $x = y$ and $q = 2$ into Equation (15). Setting x' to zero yields:

$$(1-x)\left((1-p)\,x + p\,(1-x)\right)^2 - x\left((1-p)\,(1-x) + px\right)^2 = 0 \tag{A1}$$

Factoring out and simplifying the above equation gives:

$$4px - x + p^2 + 3x^2 - 2x^3 - 12px^2 - 6p^2x + 8px^3 + 12p^2x^2 - 8p^2x^3 = 0, \tag{A2}$$

which may be written as:

$$(1-2x)\left(4px - x + p^2 + x^2 - 4px^2 - 4p^2x + 4p^2x^2\right) = 0. \tag{A3}$$

Thus:

$$4px - x + p^2 + x^2 - 4px^2 - 4p^2x + 4p^2x^2 = 0, \tag{A4}$$

and after some calculations, we arrive at:

$$x^2 - x + \frac{p^2}{(2p-1)^2} = 0. \tag{A5}$$

Solving the last equation gives:

$$x_1 = \frac{1}{2} - \frac{1}{2}\sqrt{1 - \frac{4p^2}{(2p-1)^2}}, \tag{A6}$$

$$x_2 = \frac{1}{2} + \frac{1}{2}\sqrt{1 - \frac{4p^2}{(2p-1)^2}}. \tag{A7}$$

Note that for $p > \frac{1}{4}$, both solutions are complex (i.e., the symmetric points disappear). Hence, the second transition occurs at:

$$p_2^\star = \frac{1}{4}. \tag{A8}$$

We proceed by computing the Jacobian at a symmetric point (x, x). Due to the symmetry of the dynamical system (15), the Jacobian at such a point is of the form:

$$\begin{vmatrix} a(x) & b(x) \\ b(x) & a(x) \end{vmatrix}. \tag{A9}$$

Hence, the eigenvalues are (we omit the explicit dependency on x for the sake of simplicity):

$$\lambda_1 = a + b, \tag{A10}$$
$$\lambda_2 = a - b. \tag{A11}$$

After some straightforward, but lengthy computation, we get:

$$a = (1-2p)\left(2x^2(4p-3) - 2x(4p-3) - 1 + 2p\right), \tag{A12}$$
$$b = -2p\left(2x(1-x)(1-2p) + p\right) \tag{A13}$$

Since b is negative for $p < \frac{1}{2}$, the largest eigenvalue is always $a - b$. Setting it to zero yields:

$$x^2 - x + \frac{1 + 2p^2 - 4p}{8p^2 - 16p + 6} = 0 \tag{A14}$$

Combining the last expression with Equation (A5) gives:

$$\frac{1 + 2p^2 - 4p}{8p^2 - 16p + 6} = \frac{p^2}{(2p-1)^2}, \tag{A15}$$

which is equivalent to:

$$16p^2 - 8p - 8p^3 + 1 = 0. \tag{A16}$$

We have to solve the above equation in order to get the critical value for the first transition. The relevant solution is:

$$p_1^\star = \frac{3}{4} - \frac{1}{4}\sqrt{5} \simeq 0.190\,98. \tag{A17}$$

Appendix B. Second Critical Value of p for General q

The critical value of p for the second phase transition may be calculated analytically in the case of a general q. At that critical point, the equilibrium $R_1 = (1/2, 1/2)$ changes its character from a repeller to a hyperbolic one. Hence, we have to evaluate the Jacobian at R_1 and look for a value of p, for which the smallest eigenvalue becomes zero.

The Jacobian will again have the form given by Equation (A9). Taking the derivatives of the right-hand side of Equation (15) with respect to x and y and setting $x = y = 1/2$ in the resulting expressions give:

$$a = 2q\left(\frac{1}{2}\right)^q - 2\left(\frac{1}{2}\right)^q - 2pq\left(\frac{1}{2}\right)^q, \tag{A18}$$
$$b = -pq\left(\frac{1}{2}\right)^{q-1}. \tag{A19}$$

The smallest eigenvalue of the Jacobi matrix is given by:

$$a + b = 2q\left(\frac{1}{2}\right)^q - 2\left(\frac{1}{2}\right)^q - 2pq\left(\frac{1}{2}\right)^q - pq\left(\frac{1}{2}\right)^{q-1}. \tag{A20}$$

Equating it to zero yields the critical value of p,

$$p_2^\star = \frac{2\left(\frac{1}{2}\right)^q - 2q\left(\frac{1}{2}\right)^q}{-2q\left(\frac{1}{2}\right)^q - q\left(\frac{1}{2}\right)^{q-1}} \tag{A21}$$

For $q = 2$, we obtain:

$$p_2^\star = \frac{1}{4}, \tag{A22}$$

which agrees with the result obtained in the previous section.

Appendix C. Supplementary Materials

A Jupyter notebook with Python code used for the numerical analysis of the dynamical system (15) may be found in [84].

References

1. Taber, C.S.; Lodge, M. Motivated Skepticism in the Evaluation of Political Beliefs. *Am. J. Political Sci.* **2006**, *50*, 755–769.
2. Wojcieszak, M.; Price, V. Bridging the Divide or Intensifying the Conflict? How Disagreement Affects Strong Predilections about Sexual Minorities. *Political Psychol.* **2010**, *31*, 315–339.
3. Mouw, T.; Sobel, M. Culture Wars and Opinion Polarization: The Case of Abortion. *Am. J. Sociol.* **2001**, *106*, 913–943.
4. Binder, A.R.; Dalrymple, K.E.; Brossard, D.; Scheufele, D.A. The Soul of a Polarized Democracy. *Commun. Res.* **2009**, *36*, 315–340.
5. McCright, A.M.; Dunlap, R.E. The politization of climate change and polarization in the American public's views of global warming. *Sociol. Quart.* **2011**, *52*, 2001–2010.
6. Meffert, M.F.; Chung, S.; Joiner, A.J.; Waks, L.; Garst, J. The Effects of Negativity and Motivated Information Processing During a Political Campaign. *J. Commun.* **2006**, *56*, 27–51.
7. Seeberg, P. Strategic Patience and EU Reform-Support. EU and the 'Arab Spring': The State of Play after Three Years. *Eur. Foreign Aff. Rev.* **2014**, *19*, 453–470.
8. DiMaggio, P.; Evans, J.; Bryson, B. Have American's Social Attitudes Become More Polarized? *Am. J. Sociol.* **1996**, *102*, 690–755.
9. Mäs, M.; Flache, A. Differentiation without Distancing. Explaining Bi-Polarization of Opinions without Negative Influence. *PLoS ONE* **2013**, *8*, e74516.
10. Isenberg, D.J. Group polarization: A critical review and meta-analysis. *J. Personal. Soc. Psychol.* **1986**, *50*, 1141–1151.
11. Sunstein, C.R. The Law of Group Polarization. *J. Political Philos.* **2002**, *10*, 175–195.
12. Walton, D. Bias, critical doubt, and fallacies. *Argum. Advocacy* **1991**, *28*, 1–22.
13. French, J.R.P. A formal theory of social power. *Psychol. Rev.* **1956**, *68*, 181–194.
14. Harary, F. A Criterion for Unanimity in French's Theory of Social Power. In *Studies in Social Power*; Cartwright, D., Ed.; Institute for Social Research: Ann Arbor, MI, USA, 1959; pp. 168–182.
15. Axelrod, R. The Dissemination of Culture. A Model with Local Convergence and Global Polarization. *J. Confl. Resolut.* **1997**, *41*, 203–226.
16. Hegselmann, R.; Krause, U. Opinion dynamics and bounded confidence: Models, analysis and simulation. *J. Artif. Soc. Soc. Simul.* **2002**. Available online: http://jasss.soc.surrey.ac.uk/5/3/2/2.pdf (accessed on 18 July 2017).

17. Macy, M.W.; Kitts, J.; Flache, A.; Benard, S. Polarization and Dynamic Networks. A Hopfield Model of Emergent Structure. In *Dynamic Social Network Modeling and Analysis: Workshop Summary and Papers*; Breiger, R., Carley, K., Pattison, P., Eds.; The National Academies Press: Washington, DC, USA, 2003; pp. 162–173.
18. Iyengar, S.; Hahn, K.S. Red Media, Blue Media: Evidence of Ideological Selectivity in Media Use. *J. Commun.* **2009**, *59*, 19–39.
19. Stroud, N.J. Media use and political predispositions: Revisiting the concept of selective exposure. *Political Behav.* **2008**, *30*, 341–366.
20. Stroud, N.J. Polarization and partisan selective exposure. *J. Commun.* **2010**, *60*, 556–576.
21. Knobloch-Westerwick, S.; Meng, J. Reinforcement of the political self through selective exposure to political messages. *J. Commun.* **2011**, *61*, 349–368.
22. Garrett, R.K. Politically motivated reinforcement seeking. *J. Commun.* **2009**, *59*, 676–699.
23. Garrett, R.K.; Carnahan, D.; Lynch, E. A turn toward avoidance? Selective exposure to online political information, 2004–2008. *Political Behav.* **2011**, *35*, 113–134.
24. Gentzkow, M.; Shapiro, J.M. Ideological segregation online and offline. *Quart. J. Econ.* **2011**, *126*, 1799–1839.
25. Mutz, D.C.; Mondak, J.J. The workplace as a context for cross-cutting political discourse. *J. Politics* **2006**, *68*, 140–155.
26. Price, V.; Cappella, J.N.; Nir, L. Does disagreement contribute to more deliberative opinion? *Political Commun.* **2002**, *19*, 95–112.
27. Castellano, C.; Fortunato, S.; Loreto, V. Statistical physics of social dynamics. *Rev. Mod. Phys.* **2009**, *81*, 591–646.
28. Gantert, N.; Löwe, M.; Steif, J.E. The voter model with anti-voter bonds. *Ann. l'Inst. Henri Poincare B Probab. Stat.* **2005**, *41*, 767–780.
29. Lorenz, J. A stabilization theorem for dynamics of continuous opinions. *Phys. A Stat. Mech. Appl.* **2005**, *355*, 217–223.
30. Toscani, G. Kinetic models of opinion formation. *Commun. Math. Sci.* **2006**, *4*, 481–496.
31. Brugna, C.; Toscani, G. Kinetic models of opinion formation in the presence of personal conviction. *Phys. Rev. E* **2015**, *92*, 052818.
32. Pareschi, L.; Vellucci, P.; Zanella, M. Kinetic models of collective decision making in the presence of equality bias. *Phys. A Stat. Mech. Appl.* **2017**, *467*, 201–217.
33. Albi, G.; Pareschi, L.; Zanella, M. Opinion dynamics over complex networks: Kinetic modeling and numerical methods. *Kinet. Relat. Model.* **2017**, *10*, 1–32.
34. Castellano, C.; Muñoz, M.A.; Pastor-Satorras, R. Nonlinear q-voter model. *Phys. Rev. E* **2009**, *80*, 041129.
35. Nyczka, P.; Sznajd-Weron, K. Anticonformity or Independence?—Insights from Statistical Physics. *J. Stat. Phys.* **2013**, *151*, 174–202.
36. Sznajd-Weron, K.; Szwabiński, J.; Weron, R. Is the Person-Situation Debate Important for Agent-Based Modeling and Vice-Versa? *PLoS ONE* **2014**, *9*, e112203.
37. Leifeld, P. Polarization of coalitions in an agent-based model of political discourse. *Comput. Soc. Netw.* **2014**, *1*, 1–22.
38. Abelson, R.P. Mathematical Models of the Distribution of Attitudes Under Controversy. In *Contributions to Mathematical Psychology*; Frederiksen, N., Gulliksen, H., Eds.; Rinehart Winston: New York, NY, USA, 1964; pp. 142–160.
39. Marvel, S.A.; Kleinberg, J.; Kleinberg, R.D.; Strogatz, S.H. Continuous-time model of structural balance. *Proc. Natl. Acad. Sci. USA* **2011**, *108*, 1771–1776.
40. Traag, V.A.; Dooren, P.V.; Leenheer, P.D. Dynamical Models Explaining Social Balance and Evolution of Cooperation. *PLoS ONE* **2013**, *8*, e60063.
41. Salzarulo, L. A Continuous Opinion Dynamics Model Based on the Principle of Meta-Contrast. *J. Artif. Soc. Soc. Simul.* **2006**, *9*, 13.
42. Shin, J.K.; Lorenz, J. Tipping diffusivity in information accumulation systems: More links, less consensus. *J. Stat. Mech. Theory Exp.* **2010**, *2010*, P06005.
43. Galam, S. Minority opinion spreading in random geometry. *Eur. Phys. J. B* **2002**, *25*, 403–406.
44. Mckeown, G.; Sheely, N. Mass Media and Polarisation Processes in the Bounded Confidence Model of Opinion Dynamics. *J. Artif. Soc. Soc. Simul.* **2006**, *9*, 11.

45. Albi, G.; Pareschi, L.; Zanella, M. Boltzmann–type control of opinion consensus through leaders. *Philos. Trans. R. Soc. Lond. A* **2014**, *372*, 20140138.
46. Düring, B.; Wolfram, M.T. Opinion dynamics: Inhomogeneous Boltzmann–type equations modeling opinion leadership and political segregation. *Proc. R. Soc. Lond. A* **2015**, *471*, 20150345.
47. Lee, J.K.; Choi, J.; Kim, C.; Kim, Y. Social Media, Network Heterogeneity, and Opinion Polarization. *J. Commun.* **2014**, *64*, 702–722.
48. Sunstein, C.R. *Republic.com*; Princeton University Press: Princeton, NJ, USA, 2001.
49. Van Alstyne, M.; Brynjolfsson, E. Global Village or Cyber-Balkans? Modeling and Measuring the Integration of Electronic Communities. *Manag. Sci.* **2005**, *51*, 851–868.
50. Bimber, B. The internet and political fragmentation. In *Domestic Perspectives on Contemporary Democracy*; Nardulli, P.F., Ed.; University of Illinois Press: Champaign, IL, USA, 2008; pp. 155–170.
51. Papacharissi, Z. The virtual sphere. *New Media Soc.* **2002**, *4*, 9–27.
52. Festinger, L. *A Theory of Cognitive Dissonance*; Stanford University Press: Stanford, CA, USA, 1957.
53. Klapper, J.T. *The Effects of Mass Communication*; Free Press: New York, NY, USA, 1960.
54. Delli Carpini, M.; Cook, F.L.; Jacobs, L.R. Public deliberation, discursive participation, and citizen engagement: A review of the empirical literature. *Annu. Rev. Political Sci.* **2004**, *7*, 315–344.
55. Siedlecki, P.; Szwabiński, J.; Weron, T. The interplay between conformity and anticonformity and its polarizing effect on society. *J. Artif. Soc. Soc. Simul.* **2016**, *19*, 9.
56. Liu, T.; Bundschuh, R. Quantification of the differences between quenched and annealed averaging for RNA secondary structures. *Phys. Rev. E* **2005**, *72*, 061905.
57. Myers, D.G. *Social Psychology*, 11th ed.; Freeman Press: New York, NY, USA, 2013.
58. Bond, R. Group size and conformity. *Group Process. Intergr. Relat.* **2005**, *8*, 331–354.
59. Asch, S.E. Opinions and Social Pressure. *Sci. Am.* **1955**, *193*, 31–35.
60. Conover, M.; Ratkiewicz, J.; Francisco, M.; Gonçalves, B.; Flammini, A.; Menczer, F. Political Polarization on Twitter. In Proceedings of the 5th International AAAI Conference on Weblogs and Social Media, Barcelona, Spain, 17–21 July 2011; pp. 89–96.
61. Newman, M.E.J. Modularity and community structure in networks. *Proc. Natl. Acad. Sci. USA* **2006**, *103*, 8577–8582.
62. Zachary, W. An Information Flow Model for Conflict and Fission in Small Groups. *J. Anthropol. Res.* **1977**, *33*, 452–473.
63. Sood, V.; Antal, T.; Redner, S. Voter models on heterogeneous networks. *Phys. Rev. E* **2008**, *77*, 041121.
64. Willis, R.H. Two dimensions of conformity-nonconformity. *Sociometry* **1963**, *1963*, 499–513.
65. Nail, P.R. Toward an integration of some models and theories of social response. *Psychol. Bull.* **1986**, *100*, 190–206.
66. Nail, P.R.; MacDonald, G.; Levy, D.A. Proposal of a Four Dimensional Model of Social Response. *Psychol. Bull.* **2000**, *126*, 454–470.
67. Nail, P.R.; Domenico, S.I.; MacDonald, G. Proposal of a Double Diamond Model of Social Response. *Rev. Gen. Psychol.* **2013**, *17*, 1–19.
68. Galam, S. Contrarian deterministic effects on opinion dynamics: The hung elections scenario. *Phys. A Stat. Mech. Appl.* **2004**, *333*, 453–460.
69. Krizan, Z.; Baron, R.S. Group polarization and choice-dilemmas: How important is self-categorization? *Eur. J. Soc. Psychol.* **2007**, *37*, 191–201.
70. Lewenstein, M.; Nowak, A.; Latané, B. Statistical mechanics of social impact. *Phys. Rev. A* **1992**, *45*, 763–776.
71. Stouffer, S.; Guttman, L.; Suchman, E.A.; Lazarsfeld, P.; Star, S.; Clausen, J. *Studies in Social Psychology in World War II*; Princeton University Press: Princeton, NJ, USA, 1950.
72. Guerra, P.H.C.; Meira, W., Jr.; Cardie, C.; Kleinberg, R. A Measure of Polarization on Social Media Networks Based on Community Boundaries. In Proceedings of the 7th International AAAI Conference on Web and Social Media, Cambridge, MA, USA, 8–11 July 2013; pp. 215–224.
73. Watts, D.J.; Dodds, P.S. Influentials, Networks, and Public Opinion Formation. *J. Consum. Res.* **2007**, *34*, 441–458.
74. Przybyła, P.; Sznajd-Weron, K.; Weron, R. Diffusion of innovation within an agent-based model: Spinsons, independence and advertising. *Adv. Complex Syst.* **2014**, *17*, 1450004.

75. Martín, P.V.; Bonachela, J.; Munoz, M.M. Quenched disorder forbids discontinuous transitions in nonequilibrium low-dimensional systems. *Phys. Rev. E* **2014**, *89*, 012145.
76. Malmi-Kakkada, A.N.; Valls, O.T.; Dasgupta, C. Ising model on a random network with annealed or quenched disorder. *Phys. Rev. B* **2014**, *90*, 024202.
77. Apriasz, R.; Krueger, T.; Marcjasz, G.; Sznajd-Weron, K. The hunt opinion model—An agent based approach to recurring fashion cycles. *PLoS ONE* **2016**, *11*, e0166323.
78. Knebel, J.; Weber, M.F.; Krüger, T.; Frey, E. Evolutionary games of condensates in coupled birth–death processes. *Nat. Commun.* **2015**, *6*, doi:10.1038/ncomms7977.
79. Jones, E.; Oliphant, T.; Peterson, P. SciPy: Open Source Scientific Tools for Python. Available online: http://www.scipy.org/ (accessed 18 July 2017).
80. Strogatz, S.H. *Nonlinear Dynamics and Chaos: With Applications to Physics, Biology, Chemistry, and Engineering*; Addison-Wesley: Reading, MA, USA, 1994.
81. Wise, K.; Alhabash, S.; Park, H. Emotional Responses during Social Information Seeking on Facebook. *Cyberpsychol. Behav. Soc. Netw.* **2010**, *13*, 555–562.
82. Bozdag, E. Bias in algorithmic filtering and personalization. *Ethics Inf. Technol.* **2013**, *15*, 209–227.
83. Klemm, K.; Eguíluz, V.M.; Toral, R.; Miguel, M.S. Nonequilibrium transitions in complex networks: A model of social interaction. *Phys. Rev. E* **2003**, *67*, 026120.
84. Krueger, T.; Szwabiński, J.; Weron, T. Conformity, anticonformity and polarization of opinions: Insights from a mathematical model of opinion dynamics. *arXiv* **2016**. Available online: https://doi.org/10.5281/zenodo.167817 (accessed on 18 July 2017).